DOI: 10.1002/ejic.200800287

Reactions of Halogens/Interhalogens with Polypyridyl Substrates: The Case of 2,4,6-Tris(2-pyridyl)-1,3,5-triazine

M. Carla Aragoni,[a] Massimiliano Arca,*[a] Francesco A. Devillanova,[a] Michael B. Hursthouse,[b] Susanne L. Huth,[b] Francesco Isaia,[a] Vito Lippolis,[a] Annalisa Mancini,[a] and Gaetano Verani[a]

Keywords: Halides / Interhalides / FT-Raman spectroscopy / X-ray crystal structures / Density functional calculations

---

The reactions between 2,4,6-tris(2-pyridyl)-1,3,5-triazine (tptz) and halogens (Br_2, I_2) or interhalogens (ICl, IBr) yielded different products isolated in the solid state. ($Htptz^+$)(Br_3^-), ($Htptz^+$)(IBr_2^-), (H_3tptz^{3+})($I_3Br_4^-$)(IBr_2^-)$_2$, and (H_3tptz^{3+})(ICl_2^-)$_3$, obtained from the reactions between tptz and Br_2, IBr, and ICl, were characterized by single-crystal X-ray diffraction and FT-Raman spectroscopy. All compounds are salts containing the protonated donor counterbalanced by polyhalide anions of various complexity. In particular, in (H_3tptz^{3+})($I_3Br_4^-$)(IBr_2^-)$_2$ the first example of a planar $I_3Br_4^-$ moiety can be observed. In the case of the reaction between tptz and I_2, the elemental analysis of the product indicates a 1:1 molar ratio between tptz and I_2, but the FT-Raman spectrum is not consistent with the formation of a simple adduct, clearly indicating the simultaneous presence of diiodine and symmetric triiodide.

Introduction

The design and the synthesis of novel solid-state architectures based on noncovalent interactions is among the most important targets in supramolecular and materials chemistry.[1] Since a few years ago, polyhalides, conceptually generated from the interaction between Lewis-acid-acceptor halogen molecules X_2 and Lewis base halides X^- (X = Cl, Br, I), have turned out to be very promising and flexible "building blocks" participating in the construction of novel anionic inorganic frameworks in the solid state.[2,3] It is well-established that the tendency of halogens and halides to catenate and form polyanions[4] with the general formula X^{n-}_{2m+n} ($n, m > 0$) increases on passing from chlorine to iodine. Therefore, it is not surprising that a large number of discrete polyiodides,[5] up to I_{29}^{3-},[6] and examples of infinite iodide networks[2,3] are known. These are generally formed by I^-, I_2, and I_3^- subunits interacting through I···I contacts whose distances range between 2.9 and 3.6 Å.[4] The aggregation of discrete polyiodides of this type through contacts longer than 3.6 Å up to the sum of iodine van der Waals radii (4.2 Å) can generate very intricate and fascinating infinite 3D networks.[2,7] Polybromides are far less numerous than polyiodides. Apart from Br_3^-, only linear Br_4^{2-} [isolated in ($Me_2NH_2^+$)$_2$$Br_4^{2-}$],[8] planar, Z-shaped Br_8^{2-} [isolated in (quinoclidinium$^+$)$_2$$Br_8^{2-}$],[9] and one example of an infinite polybromide 2D network[10] have been reported in the literature so far. Even fewer discrete or infinite interhalide systems have been reported.[11] Although the simplest strategy to form polyhalide architectures starts from the reaction of preformed cations with halides in the presence of different amounts of dihalogens, in most cases it is possible to start from neutral Lewis bases **L** and molecular halogens or interhalogens, since the cations can be formed in situ by either oxidation or protonation reactions of the donors. In this context, since the extension and the topology of discrete as well as extended polyhalide species largely depend upon the nature (size, shape, charge) of the templating cation,[7,13] nitrogen heterocycles represent a very flexible class of donors, because of their ease of protonation and their ability to form CT adducts. During the past few years we have been systematically testing the reactivity towards halogens and interhalogens of polypyridyl molecular substrates differing in the nature and number of nitrogen donor sites, in their dimensions, rigidity, hindrance, and directionality of bonding. We have investigated the solid-state products by X-ray diffraction and spectroscopic methods.[3,12,13] Recently, we reported on some examples of supramolecular networks obtained by reacting I_2, Br_2, IBr, and ICl with di-2-pyridyl-disulfide, tetra-2-pyridyl-pyrazine, *N*-ethyl-*N'*-3-pyridyl-imidazolidine-4,5-dione-2-thione, and *N*,*N'*-bis(3-pyridylmethyl)-imidazolidine-4,5-dione-2-thione.[3,13] Following a previous study on the construction of supramolecular architectures based on donor properties of 2,4,6-tris(2-

---

[a] Dipartimento di Chimica Inorganica ed Analitica, Università degli Studi di Cagliari,
S.S. 554 bivio per Sestu, 09042 Monserrato (Cagliari), Italy
Fax: +39-070-675-4456
E-mail: marca@unica.it
[b] School of Chemistry, University of Southampton,
Highfield, Southampton, UK, SO17 1BJ

Supporting information for this article is available on the WWW under http://www.eurjic.org or from the author.

pyridyl)-1,3,5-triazine (tptz) towards coordinatively unsaturated metal centers,[14] we report here on the solid state products obtained by reacting tptz with I_2, Br_2, IBr, and ICl.

Result and Discussion

2,4,6-Tris(2-pyridyl)-1,3,5-triazine (tptz) was treated with I_2, Br_2, IBr, and ICl in different molar ratios ranging between 1:0.5 and 1:5, to give the solid products summarized in Table 1. Only the product obtained from the reaction of tptz with diiodine was unsuitable for XRD analysis. It is worth observing that starting from tptz/halogen molar ratios lower than or equal to unity, products rich in halogen were obtained, possibly because of their particular stability in the solid state, which is determined by extended hydrogen or halogen bonding (see below).

Description of the Structures

All the products characterized by single-crystal X-ray diffraction consist of salts whose mono- or three-protonated cations, $Htptz^+$ and H_3tptz^{3+}, respectively, are counterbalanced by discrete or extended polyhalides.

The products $(Htptz^+)(Br_3^-)$ and $(Htptz^+)(IBr_2^-)$ were obtained from the reactions of tptz with dibromine and iodine monobromide, respectively, in acetonitrile. In the former (Figure 1), the charge of the monoprotonated cation is counterbalanced by a slightly asymmetric Br_3^- anion, while in the latter an almost symmetric IBr_2^- anion was found (Figure S1 in Supporting Information). In both cases, the linear trihalides feature average interatomic distances Br–Br and Br–I that are longer than the sum of the covalent radii of the constituent atoms (by 11 and 7%, respectively), in agreement with a 3c–4e description of the bond. Inspection of the crystal packing of $(Htptz^+)(Br_3^-)$ and $(Htptz^+)(IBr_2^-)$ shows that the organic cations interact with each other through hydrogen bonds of various strength. The existence of this feature in both crystal structures was confirmed by the subsequent analysis with the programme XPac.[15] In accordance with the XPac method described by Gelbrich et al., the six atoms of the triazine group C_3N_3 were chosen as the corresponding ordered set of points (COSP), and XPac analysis identified a 1D structural construct (SC), which is concurrent with the hydrogen-bonding motif of the molecular cation. As a result of the steric arrangement of $Htptz^+$, the hydrogen bonds are responsible for the formation of helixes, which propagate along the *b* axis in $(Htptz^+)(Br_3^-)$ (Figure 2) and along the *a* axis in $(Htptz^+)(IBr_2^-)$ (Figure S2 in Supporting Information). Neighboring helixes are related by translation only in the monoclinic $(Htptz^+)(Br_3^-)$ and by two 2_1 screw axes in the orthorhombic $(Htptz^+)(IBr_2^-)$. It should be noted that the direction of propagation of the SC coincides with a crystallographic 2_1 screw axis and that a 1D SC with 2_1 screw symmetry is the highest similarity possible between the space groups $P2_1$ and $P2_12_12_1$. In both $(Htptz^+)(Br_3^-)$ and $(Htptz^+)(IBr_2^-)$, further hydrogen bonds connect the monocations to the anions, the trihalides bridging symmetry-related cations.[16]

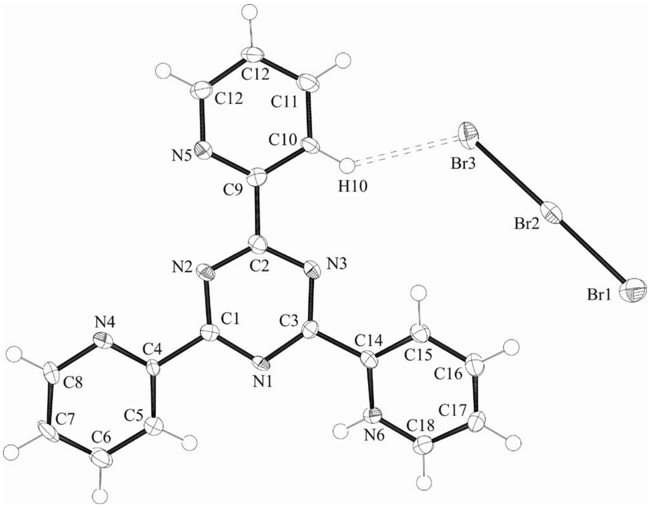

Figure 1. ORTEP drawing and atom-labeling scheme for $(Htptz^+)(Br_3^-)$. Thermal ellipsoids are shown at the 60% probability level. Bond lengths [Å] and angles [°] for the tribromide anion: Br1–Br2 2.5075(9), Br2–Br3 2.5712(9); Br1–Br2–Br3 178.99(3). Contact distance H10···Br3: 2.839 Å.

The reactions of tptz with IBr in 1:1 (v/v) ethyl acetate/dichloromethane solutions in molar ratios ranging between 1:0.5 and 1:5 always yielded the product $(H_3tptz^{3+})(I_3Br_4^-)(IBr_2^-)_2$ (Figure S3 in Supporting Information). The X-ray crystal structure established that the charge of the three-protonated cation H_3tptz^{3+}[17] is balanced by a com-

Table 1. Stoichiometry and main FT-Raman peaks (50–500 cm^{-1})[a] of the solid products obtained by reacting tptz with I_2, Br_2, IBr, and ICl.

I_2		Br_2		IBr		ICl	
Product	FT-Raman peaks	Product	FT-Raman peaks	Product	FT-Raman peaks	Product	FT-Raman peaks
Possible co-presence of $tptz{\cdot}I_2$ and $(Htptz^+)(I_3^-)$	153 (10.0) 107 (9.1)	$(Htptz^+)(Br_3^-)$ [b]	168 (10.0)	$(Htptz^+)(IBr_2^-)$ [b] $(H_3tptz^{3+})(I_3Br_4^-)(IBr_2^-)_2$ [b]	168 (10.0) 228 (10.0) 211 (5.8) 190 (8.5) 178 (4.8)	$(H_3tptz^{3+})(ICl_2^-)_3$[b]	284 (8.6) 271 (10.0)

[a] Only main peaks are reported. Relative intensities are in parentheses. [b] Crystal structure reported in this paper.

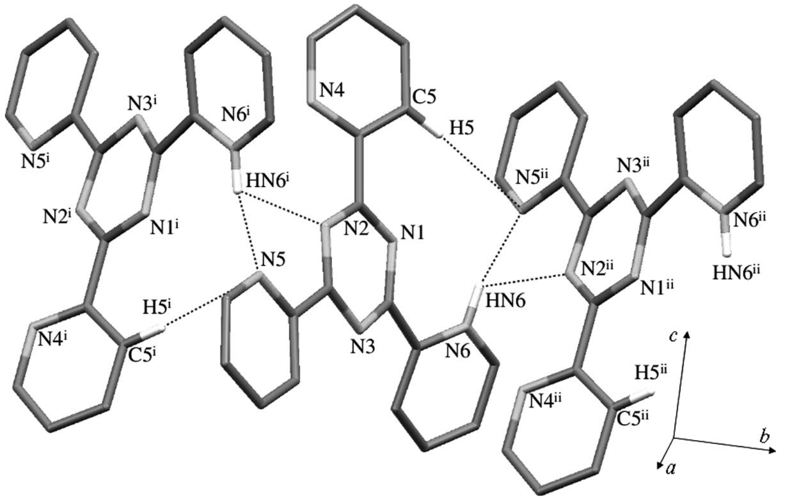

Figure 2. Hydrogen-bonding motif of ($Htptz^+$) as present in ($Htptz^+$)(Br_3^-). Only hydrogen atoms involved in hydrogen-bonding interactions are depicted for clarity. Selected contact distances [Å]: N5···H6N^{i} 1.912, N2···H6N^{i} 2.615, N5···H5^{i} 2.668. ^{i}: $-x$, $-1/2 + y$, $1 - z$; ^{ii}: $-x$, $1/2 + y$, $1 - z$.

plex polyhalide, which can be described as a planar $Br^-\cdot 3IBr$ ($I_3Br_4^-$) interacting with a IBr_2^-, disposed roughly perpendicular to the plane of $I_3Br_4^-$ (Figure 3).

The $I_3Br_4^-$ distorted planar anion can be considered to have originated from the interaction of the Br5 bromide anion with three differently perturbed IBr units [d_{I-Br} distances in the range 2.585–2.619 Å; solid state d_{I-Br} = 2.514(4) Å],[18] the central I–Br bond lengths being, as expected, longer than the terminal ones (Figure 3) and quite different from each other (in the range 2.865–3.125 Å). The unprecedented planar conformation of the $I_3Br_4^-$ anion isolated in (H_3tptz^{3+})($I_3Br_4^-$)(IBr_2^-)$_2$ renders it different from the only other previously reported example, isolated in (PPh_4^+)($I_3Br_4^-$),[19] that features a pyramidal conformation. In order to evaluate the relative stabilities of the two forms, the idealized planar and pyramidal $I_3Br_4^-$ ions (point groups D_{3h} and C_{3v}, respectively) were optimized at the

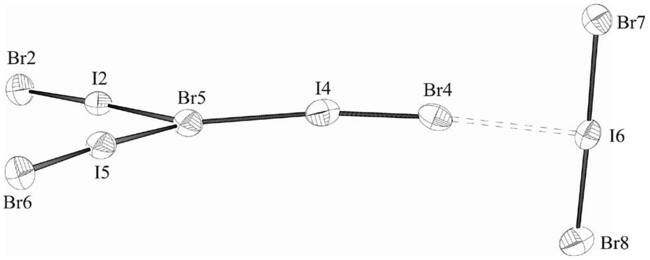

Figure 3. ORTEP drawing and atom-labeling scheme for the $I_3Br_4^-$ ion interacting with a IBr_2^- in the crystal structure of (H_3tptz^{3+})($I_3Br_4^-$)(IBr_2^-)$_2$. Thermal ellipsoids are drawn at the 60% probability level. Selected bond lengths [Å] and angles [°]: I2–Br2 2.6159(16), I4–Br4 2.6191(16), I5–Br6 2.5854(17), I2–Br5 3.0129(19), I4–Br5 3.1246(18), I5–Br5 2.8648(17), I6–Br7 2.6511(15), I6–Br8 2.7772(14), Br4···I6 3.5482(19); Br2–I2–Br5 176.74(5), Br5–I5–Br6 177.50(5), Br4–I4–Br5 171.96(5), I2–Br5–I5 92.88(4), Br7–I6–Br8 177.80(5), I4–Br4···I6 173.18(5).

Table 2. Bond lengths d_{X-Y} [Å], Wiberg bond indices W_{X-Y}, frequencies $\tilde{\nu}_R$ [cm^{-1}], and description of Raman-active vibrational modes calculated for the polyhalides discussed in the paper at the DFT/mPW1PW level.[a]

	Point group	Bond	d_{X-Y}	W_{X-Y}	$\tilde{\nu}_R$	
Br_3^- [b]	$D_{\infty h}$	Br–Br	2.628	0.516	154 σ_g	symmetric stretching mode
ICl_2^- [b]	$D_{\infty h}$	I–Cl	2.608	0.520	246 σ_g	symmetric stretching mode
IBr_2^- [b]	$D_{\infty h}$	I–Br	2.776	0.522	150 σ_g	symmetric stretching mode
I_3^- [b]	$D_{\infty h}$	I–I	2.979	0.518	108 σ_g	symmetric stretching mode
$I_3Br_4^-$	D_{3h}	I–Br (term.)[c]	2.603	0.770	221 a_1	totally symmetric combination of all in-phase terminal I–Br stretching modes
					204 e'	combination of terminal I–Br stretching modes
		I–Br (int.)[d]	2.996	0.244	127 e'	combination of internal I–Br stretching modes
$I_3Br_4^-$	C_{3v}	I–Br (term.)[c]	2.604	0.767	221 a_1	totally symmetric combination of all in-phase terminal I–Br stretching modes
					204 e	combination of terminal I–Br stretching modes
		I–Br (int.)[d]	2.997	0.252	120 e	combination of internal I–Br stretching modes

[a] LanL2DZ(d,p) basis set. [b] Optimized bond lengths and frequencies from ref.[13]. [c] Terminal I–Br distance. [d] Distance between the central bromide and the terminal IBr molecules.

DFT/mPW1PW level and their total electronic energies were calculated. Notably, optimized bond lengths within the two ions are almost identical (differing by about 1 mÅ; Table 2), but the pyramidal conformation allows for a better $n_{Br}\rightarrow\sigma^*_{I-Br}$ overlap between the filled lone pairs of the central bromide anion and the σ*-type unoccupied molecular orbitals of the coordinated IBr units, as evaluated by Wiberg bond indices (Table 2) and NBO second order perturbation theory (the main contribution accounting for 73.95 and 94.65 kcal mol^{-1} for the ions belonging to the D_{3h} and C_{3v} point groups, respectively). This notwithstanding, the entity of the charge transfer from the central bromide to the three IBr units in the pyramidal $I_3Br_4^-$ ion is almost the same (–0.214 and –0.221 *e* for each IBr in the planar and pyramidal model $I_3Br_4^-$ ions, respectively), and the D_{3h} form is less stable than the C_{3v} one by only 0.50 kcal mol^{-1}, so that even very weak intermolecular interactions must be capable of controlling the final geometry of the system.

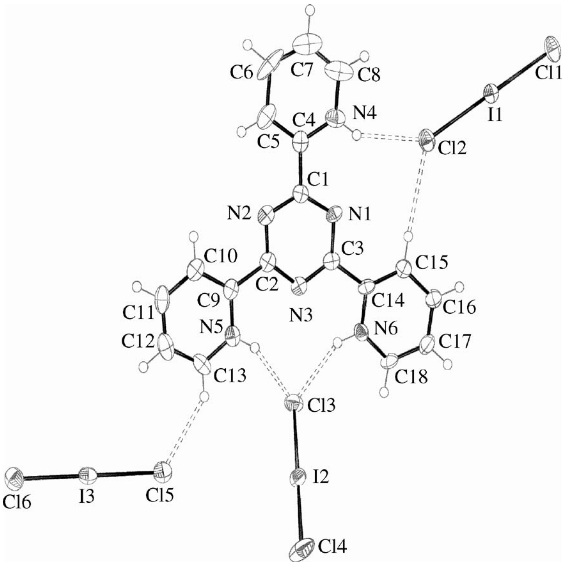

Figure 4. ORTEP drawing and atom-labeling scheme for $(H_3tptz^{3+})(ICl_2^-)_3$. Thermal ellipsoids are drawn at the 60% probability level. Selected bond lengths [Å] and angles [°]: I1–Cl1 2.515(2), I1–Cl2 2.595(2), I2–Cl3 2.623(2), I2–Cl4 2.472(3), I3–Cl5 2.585(3), I3–Cl6 2.492(2), Cl3···H5N 2.360, Cl3···H6N 2.332, Cl5···H13 2.569, Cl2···H4N 2.484, Cl2···H15 2.815; Cl1–I1–Cl2 178.23(7), Cl3–I2–Cl4 178.30(8), Cl5–I3–Cl6 178.63(8).

The reaction of tptz and ICl in the explored molar ratios yielded the salt $(H_3tptz^{3+})(ICl_2^-)_3$, featuring the three-protonated cation H_3tptz^{3+} counterbalanced by three slightly asymmetric ICl_2^- linear anions (Figure 4). It is worth noting that the cation is almost planar, the mean plane being perpendicular to the *c* axis. Two of the counterbalancing ICl_2^- anions also lie in the *ab* plane and form hydrogen bonds bridging symmetry-related cations to form a sheetlike arrangement parallel to the *ab* plane (Figure 5a). The third ICl_2^- anion is situated between the sheets. The chlorine atoms point at the pockets formed by N5, N3, N6 and C5, N2, C10 in neighboring sheets, thus directing the stacking of the cation sheets along the *c* axis (Figure 5b).

FT-Raman Spectra

FT-Raman spectroscopy in the near-infrared region (50–500 cm^{-1}) has proved to be a tool of particular help in providing qualitative as well as quantitative structural information for the compounds obtained by reacting molecular donors with diiodine,[20] and correlations between structural features and vibrational properties were obtained by the analysis of a large number of crystallographically characterized compounds.[20–23] In the case of weak or medium–weak diiodine adducts, the charge transfer from the donor to the diiodine moiety is reflected in the lowering of the frequency, $\tilde{\nu}_{I-I}$, of the Raman-active I–I stretching vibration with respect to that measured in the free dihalogen. In the case of polyiodides, FT-Raman spectroscopy has been extensively used to provide structural information on their I_2 and I_3^- building blocks, while it is not capable of clearly

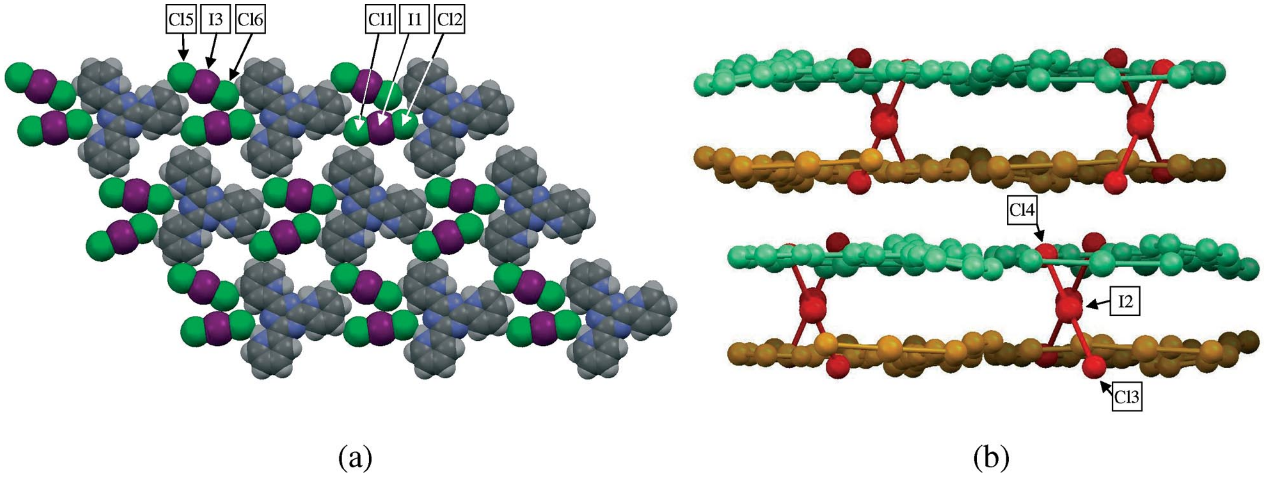

Figure 5. (a) Space-filling view of the sheet formed in the *ab* plane by the H_3tptz^{3+} cations bridged by ICl_2^- anions in (H_3tptz^{3+})-$(ICl_2^-)_3$. (b) The third ICl_2^- connects parallel sheets stacked along the *c* vector. Cl6···H16^{i} 2.576, H11^{ii}···Cl1 2.728, H10^{iii}···Cl4 2.644 Å. ^{i}: *x*, 1 + *y*, *z*; ^{ii}: *x*, –1 + *y*, *z*, ^{iii}: –*x*, 1/2 + *y*, 1/2 – *z*.

distinguishing between the possible extended structures formed by these subunits.[5,24] The literature on FT-Raman spectroscopy measurements, which is rich on the topics diiodine and polyiodides, is indeed much poorer as far as interhalogens and interhalides are concerned. Thus, the harvesting of FT-Raman spectroscopic data on systems containing interhalides and the comparison with their structural features is of great importance in establishing the same extent of structure–property relationships largely acknowledged for diiodine and (poly)iodides. In this context, FT-Raman spectroscopy can be confidently exploited for investigating the nature of the solid product isolated from the reaction between tptz and diiodine, while the comparison of the structural features of the products obtained from the reactions with Br_2, IBr, and ICl (Table 1) with the FT-Raman spectroscopic information allows to expand the knowledge-base on the Raman spectroscopic response of structurally known polyhalides and interhalides. In addition, the assignment of the experimental FT-Raman peaks can be corroborated by the results of normal-mode frequency calculations carried out at the DFT/mPW1PW level on all the species suggested by the elemental or XRD analyses of the isolated reaction products (Table 2).

Although elemental analysis of the compound obtained by reacting tptz and I_2 is in agreement with a 1:1 molar ratio between tptz and I_2, the product must not be a simple adduct. In fact, the FT-Raman spectrum (Figure 6a) features two peaks at 153 and 107 cm^{-1}. While the former indicates the presence of an elongated diiodine unit, possibly perturbed by a CT interaction with the nitrogen donor (solid-state I_2: $d_{\text{I–I}} = 2.715$ Å; $\tilde{\nu}_{\text{I–I}} = 180\ cm^{-1}$),[21,25] the latter is certainly due to a symmetric I_3^- anion, since symmetric linear triiodides (point group $D_{\infty h}$) feature a single Raman-active mode due to the σ_g stretching vibration at about 110 cm^{-1} (calculated at 108 cm^{-1}, Table 2). Thus, both symmetric I_3^- and perturbed I_2 species are simultaneously present in the solid product, as previously reported in different systems.[26]

$(Htptz^+)(Br_3^-)$ and $(Htptz^+)(IBr_2^-)$ have FT-Raman spectra with similar features. In the case of $(Htptz^+)(Br_3^-)$, the FT-Raman spectrum is dominated by an intense peak at 168 cm^{-1} (Figure 6b) that can be assigned to the σ_g stretching mode of the trihalide (calculated at $\tilde{\nu}_{\text{Br–Br}} = 154\ cm^{-1}$ for a symmetric Br_3^-, point group $D_{\infty h}$; Table 2). The FT-Raman spectrum of $(Htptz^+)(IBr_2^-)$ also features an intense peak at 168 cm^{-1} due to σ_g stretching mode of a symmetric IBr_2^- anion, calculated at 150 cm^{-1}.[13] In the FT-Raman spectra of both compounds, the absence of well visible peaks at about 190 cm^{-1} agrees with the fairly symmetric nature of the two trihalides.

The FT-Raman spectrum of $(H_3tptz^{3+})(I_3Br_4^-)(IBr_2^-)_2$ shows a large number of peaks in the range 150–250 cm^{-1}

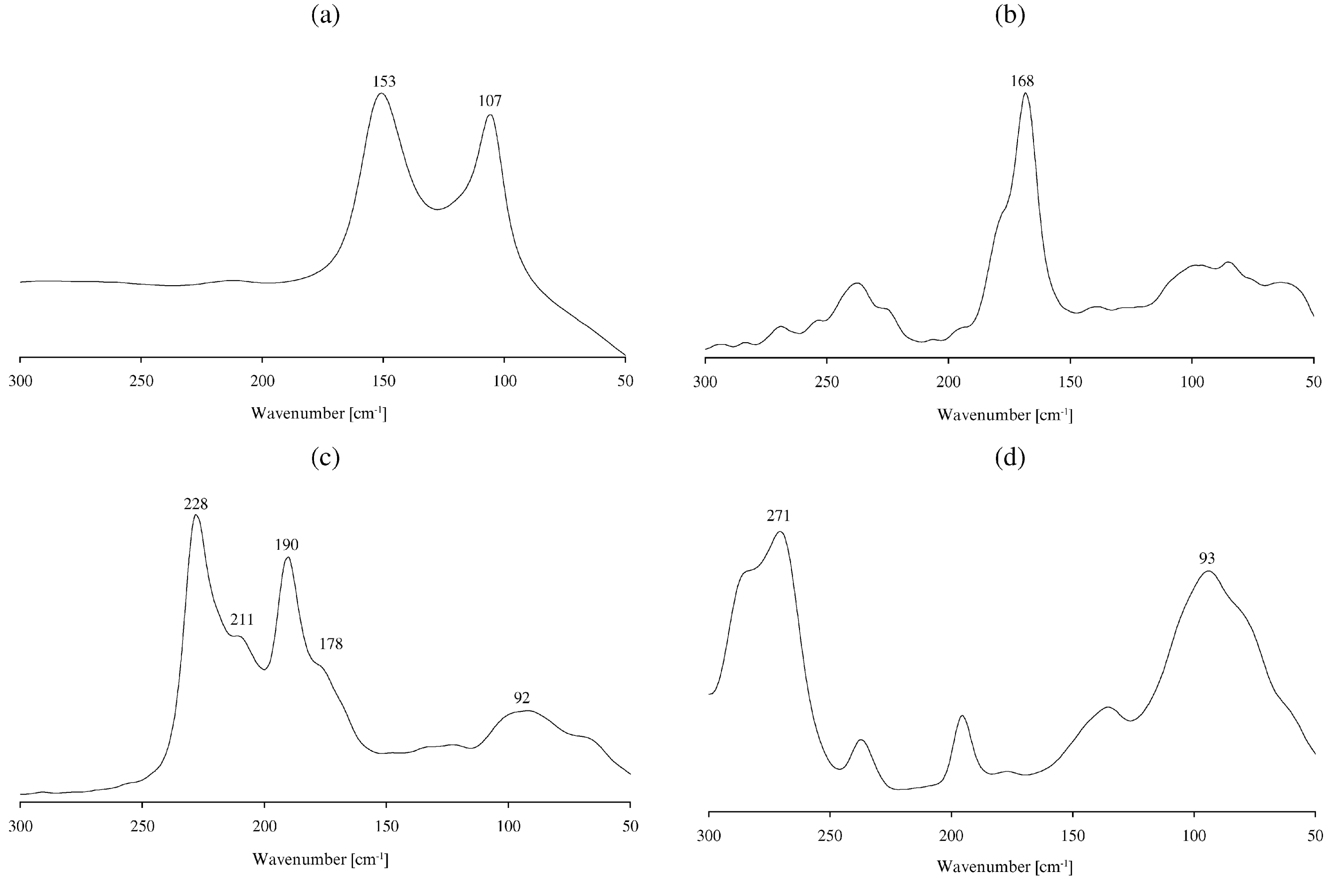

Figure 6. FT-Raman spectrum (300–50 cm^{-1}, solid state) of (a) the solid-state product obtained by reacting tptz with diiodine, (b) $(Htptz^+)(Br_3^-)$, (c) $(H_3tptz^{3+})(I_3Br_4^-)(IBr_2^-)_2$, and (d) $(H_3tptz^{3+})(ICl_2^-)_3$.

(Figure 6c). A comparison of this spectrum with that previously reported for the only other example of the $I_3Br_4^-$ anion, isolated in $(PPh_4^+)(I_3Br_4^-)$,[19] shows many similarities. Indeed, notwithstanding the different conformations of $I_3Br_4^-$, which adopts either a planar or a pyramidal shape in $(H_3tptz^{3+})(I_3Br_4^-)(IBr_2^-)_2$ or $(PPh_4^+)(I_3Br_4^-)$, respectively, the energies of the corresponding normal modes are calculated to be very similar (Table 2). The main peak at 228 cm^{-1} can be attributed to the totally symmetric combination of the in-phase stretching modes of the three perturbed IBr units of the $I_3Br_4^-$ anion, calculated just at the same wavenumber for an idealized model anion belonging to the D_{3h} point group (gas phase $d_{\text{I–Br}}$ = 2.485 Å, $\tilde{\nu}_{\text{I–Br}}$ = 267 cm^{-1}).[27] The e' combination of the same stretching modes is calculated at 204 cm^{-1} and can be tentatively envisaged in the peaks at 211 and 190 cm^{-1} in the experimental FT-Raman spectrum, the two bands possibly originating from the nonequivalence of the IBr units, resulting in a symmetry descent of the combinations. The e' combination of the vibrational modes involving the central bromide and the coordinated IBr molecule of the $I_3Br_4^-$ ion is calculated at 127 cm^{-1} and can be identified in the broad weak peak at about 130 cm^{-1}. Finally, the symmetric stretching modes of the IBr_2^- ions, at 168 cm^{-1} for $(Htptz^+)(IBr_2^-)$, can be envisaged in the shoulder of the peak at 190 cm^{-1}, located at about 178 cm^{-1}.

In $(H_3tptz^{3+})(ICl_2^-)_3$, the three-protonated cation is balanced by three ICl_2^- anions: the strong FT-Raman peak envelope at about 280 cm^{-1} (Figure 6d) agrees well with the presence of the three slightly different ICl_2^- anions and can be attributed to the overlap of their stretching vibrations.[13] This assignment is consistent with those previously reported for salts of the type $[\mathbf{L}_2I^+]ICl_2^-$ and $(H_3\mathbf{L}^{3+})(ICl_2^-)_3$ (**L** = 2-methylpyridine, 1,10-phenanthroline, and tetra-2-pyridylpyrazine), for which the reported Raman peak positions were 265, 269, and 270 cm^{-1}, respectively.[13,28]

Conclusions

The solid-state products obtained from the reactions between tptz and I_2, Br_2, IBr, and ICl were investigated. Both X-ray diffraction analysis and FT-Raman spectroscopy were exploited for the understanding of their nature. The literature reports clearly defined relationships between structural features and FT-Raman spectroscopic responses only in the case of the products obtained from the reactions of diiodine and N, S, or Se-donors.[20,21] On the contrary, the reports on FT-Raman spectroscopic data collected on compounds containing derivatives of dibromine and interhalogens are much fewer. In this context, the collection of structural data on all compounds obtained from the reactions between tptz and Br_2, IBr, and ICl represents an important step in increasing the knowledge regarding the FT-Raman spectroscopic response of structurally known halogen assemblies. The combined use of both techniques confirmed that (poly)pyridyl substrates can be made to react with halogens and interhalogens to give either CT adducts or pyridinium cations balanced by halide or polyhalide anions. As regards the product isolated from the reaction between tptz and molecular iodine, where crystals suitable for X-ray diffraction analysis were not available, FT-Raman spectroscopy indicates the co-presence of perturbed diiodine molecules and triiodides: obviously, the structural features of the product, consistent with a mixture of a CT adduct and a triiodide salt, could only be hypothesized. In all other cases, *N*-protonated ionic products counterbalanced by discrete or extended halides were the only products isolated. It is worthy of note that the first example of a structurally characterized planar $I_3Br_4^-$ was obtained.

Finally, on the basis of the existing literature, the results reported in this paper, and the recent structural characterizations of $[(H_4tppz^{4+})(Br^-)_2(Br_4^{2-})]$[12] and $[(Hdps^+)(I^-)\cdot 5/2I_2]$[3] [tppz = tetra(2-pyridyl)pyrazine and dps = bis(2-pyridyl)disulfide], pyridyl substrates seem to represent a very flexible class of compounds, capable of stabilizing a great variety of different polyhalide anions in often fascinating supramolecular networks.

Experimental Section

General Considerations: All solvents and reagents were purchased from Aldrich and used without further purification. $CHCl_3$ and CH_2Cl_2 were freshly distilled over $LiAlH_4$ prior to use. Elemental analyses were performed with a FISONS EA-1108 CHNS-O instrument. Infrared spectra were recorded with a Bruker IFS55 spectrometer at room temperature, by purging the sample cell with a flow of dried air. Polythene pellets with a Mylar beam-splitter and polythene windows (50–500 cm^{-1}, resolution 2 cm^{-1}) and KBr pellets with a KBr beam-splitter and KBr windows (400–4000 cm^{-1}, resolution 4 cm^{-1}) were used. FT-Raman spectra, in the range 50–500 cm^{-1}, were recorded with a resolution of 2 cm^{-1} by using a Bruker RFS100 FT-Raman spectrometer fitted with an In-Ga-As detector (room temperature) operating with a Nd-YAG laser (excitation wavelength 1064 nm; 100 mW) with a 180° scattering geometry. X-ray structure determination and crystallographic data (summarized in Table 3) for $(Htptz^+)(Br_3^-)$, $(Htptz^+)(IBr_2^-)$, $(H_3tptz^{3+})(I_3Br_4^-)(IBr_2^-)_2$, and $(H_3tptz^{3+})(ICl_2^-)_3$ were collected at 120(2) K by means of combined phi and omega scans with a Bruker Nonius KappaCCD area detector situated at the window of a rotating anode (graphite Mo-K_α radiation, λ = 0.71073 Å). The structures were solved by direct methods with SHELXS-97 and refined on F^2 by using SHELXL-97.[29] Anisotropic displacement parameters were assigned to all non-hydrogen atoms. Hydrogen atoms were included in the refinement, but thermal parameters and geometry were constrained to ride on the atom to which they were bonded. CCDC-690511, -690512, -690513, and -690514 contain the supplementary crystallographic data for this paper. These data can be obtained free of charge from The Cambridge Crystallographic Data Centre via www.ccdc.cam.ac.uk/data_request/cif. The organic solutions of halogens and interhalogens were previously titrated by suspending 1 mL of solution in 50 mL of bidistilled water, adding excess KI, and titrating with a standard solution of sodium thiosulfate (0.01 M) with a Metrohm 776 Dosimat automatic buret. Density functional theory (DFT) calculations were performed with Gaussian03[30] as described previously,[13] exploiting the mPW1PW functional[31] and the LanL2DZdp basis set with ECP,[32,33] including diffuse and polarization functions.[34]

Table 3. Crystal data for $(Htptz^+)(Br_3^-)$, $(Htptz^+)(IBr_2^-)$, $(H_3tptz^{3+})(I_3Br_4^-)(IBr_2^-)_2$, and $(H_3tptz^{3+})(ICl_2^-)_3$.[a]

	$(Htptz^+)(Br_3^-)$	$(Htptz^+)(IBr_2^-)$	$(H_3tptz^{3+})(I_3Br_4^-)(IBr_2^-)_2$	$(H_3tptz^{3+})(ICl_2^-)_3$
Empirical formula	$C_{18}H_{13}N_6Br_3$	$C_{18}H_{13}N_6I_1Br_2$	$C_{18}H_{15}N_6I_5Br_8$	$C_{18}H_{15}N_6I_3Cl_6$
Crystal size [mm]	0.45 × 0.40 × 0.36	0.60 × 0.46 × 0.25	0.46 × 0.04 × 0.02	0.10 × 0.04 × 0.02
Crystal system	monoclinic	orthorhombic	triclinic	orthorhombic
Space group	$P2_1$	$P2_12_12_1$	$P1$	$Pbca$
a [Å]	9.12740(10)	10.9213(8)	8.156(2)	22.649(15)
b [Å]	10.4278(2)	11.8985(7)	14.103(4)	18.448(10)
c [Å]	10.3005(2)	14.8920(11)	16.380(6)	13.240(7)
α [°]	90	90	90.94(2)	90
β [°]	99.5380(10)	90	99.31(2)	90
γ [°]	90	90	100.91(2)	90
V [Å^3]	966.84(3)	1935.2(2)	1823.5(10)	5532(6)
Z	2	4	2	8
D_{calc} [Mg m^{-3}]	1.900	2.060	2.894	2.182
Independent reflections	4275	4408	8315	6324
Number of parameters	245	245	338	299
Final $R1$ [b]	0.0486	0.0489	0.0516	0.0573
$wR2$ (all data)	0.1304	0.1265	0.1024	0.0915

[a] T = 120(2) K; wavelength Mo-K_α (0.71073 Å). [b] $[F^2 > 2\sigma(F^2)]$.

NBO populations[35] and Wiberg bond indices[36] were calculated at the optimized geometries.

Synthesis and Characterization: All products were obtained according to the following procedure: a solution (solvents are specified in each preparation) of a weighted amount of tptz (25 mg, 8.0×10^{-5} mol) was made to react with a previously titrated solution of the halogen (I_2, Br_2) or interhalogen (IBr, ICl) in 1:0.5, 1:1, 1:2, and 1:5 molar ratios. The solution was allowed to concentrate slowly in air. After a few days, the solid product was separated and washed with light petroleum ether (b.p. 40–60 °C).

Reaction of tptz and I_2 (in CH_2Cl_2): M.p. 233–236 °C (decomposition). $C_{18}H_{12}I_2N_6$ (566.14): calcd. C 38.19, H 2.14, N 14.84; found C 38.29, H 2.53, N 14.93. Solid-state FTIR: $\tilde{\nu}$ = 3050 (w), 1573 (w), 1524 (s), 1469 (w), 1373 (s), 1257 (m), 1149 (m), 1092 (m), 1045 (m), 1001 (m), 852 (w), 767 (s), 733 (w), 667 (w), 624 (m), 491 (s), 452 (m), 402 (s), 294 (s), 260 (m), 240 (m), 217 (w), 184 (m), 162 (s), 145 (s), 75 (s) cm^{-1}. FT-Raman spectrum (50 mW; relative intensities in parentheses, strongest = 10): 153 (10.0), 107 (9.1) cm^{-1}.

Reaction of tptz and Br_2 (in CH_3CN): M.p. > 250 °C. $C_{18}H_{13}Br_3N_6$ (553.05): calcd. C 39.09, H 2.37, N 15.20; found C 39.56, H 2.31, N 15.11. Solid-state FTIR: $\tilde{\nu}$ = 3421 (w), 2360 (w), 1700 (w), 1653 (m), 1631 (w), 1624 (m), 1517 (s), 1473 (m), 1371 (s), 1287 (w), 1261 (w), 1146 (m), 1048 (m), 1009 (m), 768 (s), 665 (m), 597 (m), 494 (m), 466 (m), 423 (w), 403 (m), 332 (w), 309 (m), 296 (m), 271 (w), 250 (w), 234 (m), 191 (s), 164 (s), 144 (s), 115 (s), 94 (s), 64 (s) cm^{-1}. FT-Raman spectrum (50 mW; relative intensities in parentheses, strongest = 10): 238 (6.7), 168 (10.0), 97 (7.0) cm^{-1}.

Reaction of tptz and IBr (in CH_2Cl_2): M.p. > 250 °C. $C_{18}H_{13}Br_2IN_6$ (600.05): calcd. C 36.03, H 2.18, N 14.01; found C 35.75, H 1.94, N 13.93. Solid-state FTIR: $\tilde{\nu}$ = 3444 (w), 2915 (w), 2369 (w), 1643 (m), 1625 (w), 1585 (w), 1571 (m), 1533 (s), 1423 (m), 1334 (s), 1287 (m), 1238 (m), 1222 (m), 1155 (m), 1090 (m), 1030 (m), 1010 (m), 996 (m), 791 (s), 661 (m), 634 (m), 488 (w) cm^{-1}. FT-Raman spectrum (50 mW; relative intensities in parentheses, strongest = 10): 168 (10.0), 85 (2.8), 64 (2.2) cm^{-1}.

Reaction of tptz and IBr (in 1:1 v/v ethyl acetate/CH_2Cl_2): M.p. > 250 °C. $C_{18}H_{15}Br_8I_5N_6$ (1589.11): calcd. C 13.60, H 0.95, N 5.29; found C 13.85, H 1.14, N 4.93. Solid-state FTIR: $\tilde{\nu}$ = 3534 (w), 2930 (w), 2591 (w), 1639 (w), 1631 (m), 1589 (m), 1521 (s), 1401 (m), 1363 (s), 1241 (m), 1212 (m), 1176 (m), 1023 (m), 1010 (m), 981 (m), 744 (s), 631 (m), 401 (w) cm^{-1}. FT-Raman spectrum (50 mW; relative intensities in parentheses, strongest = 10): 228 (10.0), 211 (5.8), 190 (8.5), 178 (4.8), 93 (3.2) cm^{-1}.

Reaction of tptz and ICl (in $CHCl_3$ or CH_2Cl_2): M.p. > 250 °C. $C_{18}H_{15}Cl_6I_3N_6$ (908.79): calcd. C 23.79, H 1.66, N 9.25; found C 23.95, H 1.63, N 9.15. Solid-state FTIR: $\tilde{\nu}$ = 3088 (m), 2502 (m), 1612 (m), 1591 (w), 1543 (w), 1515 (s), 1371 (s), 1300 (m), 1261 (m), 1226 (m), 1147 (m), 1089 (m), 1047 (m), 1009 (m), 995 (m), 851 (m), 812 (w), 799 (w), 766 (s), 665 (m), 631 (m), 596 (m), 489 (m), 438 (s), 383 (m), 326 (w), 280 (s), 234 (m), 218 (m), 185 (m), 121 (m), 58 (m) cm^{-1}. FT-Raman spectrum (50 mW; relative intensities in parentheses, strongest = 10): 284 (8.6), 271 (10.0), 238 (2.5), 196 (3.4), 136 (3.7), 93 (8.6) cm^{-1}.

Supporting Information (see footnote on the first page of this article): Molecular ORTEP scheme and supramolecular hydrogen-bonding motif for $(Htptz^+)(IBr_2^-)$, and the molecular structure of $(H_3tptz^{3+})(I_3Br_4^-)(IBr_2^-)_2$.

---

[1] a) J. M. Lehn, *Supramolecular Chemistry: Concepts and Perspectives*, VCH Verlag, Weinheim, **1995**; b) F. Vogtle, *Supramolecular Chemistry*, Wiley, Chichester, **1971**; c) G. Desiraju, *Chem. Commun.* **2005**, 2995–3001; d) B. Moulton, B. Zaworotko, *Chem. Rev.* **2001**, *101*, 1629–1658.

[2] A. J. Blake, F. A. Devillanova, R. O. Gould, W.-S. Li, V. Lippolis, S. Parson, C. Radek, M. Schröder, *Chem. Soc. Rev.* **1998**, *27*, 195–206.

[3] M. C. Aragoni, M. Arca, F. A. Devillanova, M. B. Hursthouse, S. L. Huth, F. Isaia, V. Lippolis, A. Mancini, *CrystEngComm* **2004**, *6*, 540–542.

[4] P. H. Svensson, L. Kloo, *Chem. Rev.* **2003**, *103*, 1649–1684.

[5] M. C. Aragoni, M. Arca, F. Demartin, F. A. Devillanova, A. Garau, F. Isaia, V. Lippolis, S. Rizzato, G. Verani, *Inorg. Chim. Acta* **2004**, *357*, 3803–3809.

[6] K.-F. Tebbe, R. Buchem, *Angew. Chem. Int. Ed. Engl.* **1997**, *36*, 1345–1346.

[7] C. J. Horn, A. J. Blake, N. R. Champness, A. Garau, V. Lippolis, C. Wilson, M. Schröder, *Chem. Commun.* **2003**, 312–313.

[8] K. O. Strømme, *Acta Chem. Scand.* **1959**, *13*, 2089–2090.

[9] K. N. Robertson, P. K. Bakshi, T. S. Cameron, O. Knop, *Z. Anorg. Allg. Chem.* **1997**, *623*, 104–114.

[10] M. C. Aragoni, M. Arca, F. A. Devillanova, F. Isaia, V. Lippolis, A. Mancini, L. Pala, A. M. Z. Slawin, J. D. Woollins, *Chem. Commun.* **2003**, 2226–2227.

[11] a) A. Parlow, H. Hartl, *Acta Crystallogr., Sect. B* **1979**, *35*, 1930–1933; b) A. Parlow, H. Hartl, *Z. Naturforsh.* **1985**, *40*, 40–45.

[12] M. C. Aragoni, M. Arca, F. A. Devillanova, M. B. Hursthouse, S. L. Huth, F. Isaia, V. Lippolis, A. Mancini, H. R. Ogilvie, *Inorg. Chem. Commun.* **2005**, *8*, 79–82.

[13] M. C. Aragoni, M. Arca, F. A. Devillanova, M. B. Hursthouse, S. L. Huth, F. Isaia, V. Lippolis, A. Mancini, H. R. Ogilvie, G. Verani, *J. Organomet. Chem.* **2005**, *690*, 1923–1933.

[14] M. C. Aragoni, M. Arca, F. A. Devillanova, M. B. Hursthouse, S. L. Huth, F. Isaia, V. Lippolis, A. Mancini, S. Soddu, G. Verani, *Dalton Trans.* **2007**, 2127–2134.

[15] T. Gelbrich, M. B. Hursthouse, *CrystEngComm* **2005**, *7*, 324–336.

[16] (Htptz$^+$)(Br$_3^-$): H10···Br3 2.839, Br3···H7^{iii} 2.929, Br3···H13^{iv} 2.957 Å, ^{iii} = 1 + *x*, *y*, –1 + *z*, ^{iv} = 1 –*x*, 1/2 + *y*, 1 –*z*; (Htptz$^+$)(IBr$_2^-$): Br1···H16 2.950, Br1···H15 2.861, Br1···H12^{iv} 2.808, Br1···H18^{v} 2.931, ^{iv} = *x*, *y*, –1 + *z*, ^{v} = 1 –*x*, –1/2 + *y*, 1/2 –*z*.

[17] It is worth noting that the cation H$_3$tptz^{3+} adopts a nearly planar conformation as opposed to the distortion found in the singly protonated cation Htptz$^+$ isolated in (Htptz$^+$)(Br$_3^-$) and (Htptz$^+$)(IBr$_2^-$). In the crystal assembly, each H$_3$tptz^{3+} moiety is "sandwiched" between two I$_3$Br$_4^-$ polyhalides, so that the centroids of the cation and one of the anions match almost perfectly, while the centroid of the second I$_3$Br$_4^-$ anion is shifted with respect to the cation. The remaining anions are all IBr$_2^-$ ions occupying positions perpendicular to this sandwich complex and thus maximizing the interactions between the bromine atoms and the three clefts of the cation.

[18] L. N. Swink, G. B. Carpenter, *Acta Crystallogr., Sect. B* **1968**, *24*, 429–433.

[19] R. Minkwitz, M. Berkei, R. Ludwig, *Inorg. Chem.* **2001**, *40*, 25–28.

[20] M. C. Aragoni, M. Arca, F. A. Devillanova, A. Garau, F. Isaia, V. Lippolis, A. Mancini, G. Verani, *Bioinorg. Chem. Appl.* **2006**, Article ID 58937.

[21] P. Deplano, J. R. Ferraro, M. L. Mercuri, E. F. Trogu, *Coord. Chem. Rev.* **1999**, *188*, 71–95.

[22] P. Klaboe, *J. Am. Chem. Soc.* **1967**, *89*, 3667–3676.

[23] P. Deplano, F. A. Devillanova, J. Ferraro, M. L. Mercuri, V. Lippolis, E. F. Trogu, *Appl. Spectrosc.* **1994**, *48*, 236–240.

[24] P. Deplano, F. A. Devillanova, J. R. Ferraro, F. Isaia, V. Lippolis, M. L. Mercuri, *Appl. Spectrosc.* **1992**, *46*, 1625–1629.

[25] F. van Bolhuis, P. B. Kotter, T. Migchelsen, *Acta Crystallogr.* **1967**, *23*, 90–91.

[26] a) L. R. Gray, S. J. Higgins, W. Levason, M. Webster, *J. Chem. Soc., Dalton Trans.* **1984**, 1433–1439; b) S. Lee, B. Chen, D. C. Fredrickson, F. J. Di Salvo, E. Lebkowsky, J. A. Adams, *Chem. Mater.* **2003**, *15*, 1420–1433.

[27] a) B. Rosen (Ed.), *Spectroscopic Data Relative to Diatomic Molecules*, Pergamon, New York, **1970**; b) C. A. Wight, B. S. Ault, L. Andrews, *J. Mol. Spectrosc.* **1975**, *56*, 239–250.

[28] G. A. Bowmaker, K. H. Tan, M. J. Taylor, *Aust. J. Chem.* **1980**, *33*, 1743–1751.

[29] G. M. Sheldrick, *SHELX Suite of Programs for Crystal Structure Solution and Refinement*, University of Göttingen, Germany, **1997**.

[30] M. J. Frisch, G. W. Trucks, H. B. Schlegel, G. E. Scuseria, M. A. Robb, J. R. Cheeseman, J. A. Montgomery Jr., T. Vreven, K. N. Kudin, J. C. Burant, J. M. Millam, S. S. Iyengar, J. Tomasi, V. Barone, B. Mennucci, M. Cossi, G. Scalmani, N. Rega, G. A. Petersson, H. Nakatsuji, M. Hada, M. Ehara, K. Toyota, R. Fukuda, J. Hasegawa, M. Ishida, T. Nakajima, Y. Honda, O. Kitao, H. Nakai, M. Klene, X. Li, J. E. Knox, H. P. Hratchian, J. B. Cross, V. Bakken, C. Adamo, J. Jaramillo, R. Gomperts, R. E. Stratmann, O. Yazyev, A. J. Austin, R. Cammi, C. Pomelli, J. W. Ochterski, P. Y. Ayala, K. Morokuma, G. A. Voth, P. Salvador, J. J. Dannenberg, V. G. Zakrzewski, S. Dapprich, A. D. Daniels, M. C. Strain, O. Farkas, D. K. Malick, A. D. Rabuck, K. Raghavachari, J. B. Foresman, J. V. Ortiz, Q. Cui, A. G. Baboul, S. Clifford, J. Cioslowski, B. B. Stefanov, G. Liu, A. Liashenko, P. Piskorz, I. Komaromi, R. L. Martin, D. J. Fox, T. Keith, M. A. Al-Laham, C. Y. Peng, A. Nanayakkara, M. Challacombe, P. M. W. Gill, B. Johnson, W. Chen, M. W. Wong, C. Gonzalez, and J. A. Pople, *Gaussian 03*, Gaussian, Inc., Wallingford CT, **2004**.

[31] C. Adamo, V. Barone, *J. Chem. Phys.* **1998**, *104*, 664–675.

[32] P. J. Way, W. R. Wadt, *J. Chem. Phys.* **1985**, *82*, 299–310.

[33] J. V. Ortiz, P. J. Hay, R. L. Martin, *J. Am. Chem. Soc.* **1992**, *114*, 2736–2737.

[34] Basis sets were obtained from the Extensible Computational Chemistry Environment Basis Set Database, Version 02/02/06, as developed and distributed by the Molecular Science Computing Facility, Environmental and Molecular Sciences Laboratory which is part of the Pacific Northwest Laboratory, P. O. Box 999, Richland, Washington 99352, USA, and funded by the U. S. Department of Energy. The Pacific Northwest Laboratory is a multi-program laboratory operated by Battelle Memorial Institute for the U. S. Department of Energy under contract DE-AC06–76RLO 1830. Contact Karen Schuchardt for further information.

[35] a) A. E. Reed, F. Weinhold, *J. Chem. Phys.* **1983**, *78*, 4066–4073; b) A. E. Reed, R. B. Weinstock, F. Weinhold, *J. Chem. Phys.* **1985**, *83*, 735–746; c) A. E. Reed, L. A. Curtiss, F. Weinhold, *Chem. Rev.* **1988**, *88*, 899–926.

[36] K. Wiberg, *Tetrahedron* **1968**, *24*, 1083–1096.

Received: March 18, 2008